Available online at www.sciencedirect.com
ScienceDirect
Journal of Solid State Chemistry 180 (2007) 432–439
JOURNAL OF SOLID STATE CHEMISTRY
www.elsevier.com/locate/jssc

Synthesis and single crystal structures of ternary phosphides Li_4SrP_2 and $AAePP$ (A = Li, Na; Ae = Sr, Ba)

Yongkwan Dong, Francis J. DiSalvo*

Baker Laboratory, Department of Chemistry and Chemical Biology, Cornell University, Ithaca, NY 14853-1301, USA

Received 18 August 2006; received in revised form 23 October 2006; accepted 30 October 2006
Available online 10 November 2006

Abstract

Two new (NaSrP, Li_4SrP_2) and two known (LiSrP, LiBaP) ternary phosphides have been synthesized and characterized using single crystal X-ray diffraction studies. NaSrP crystallizes in the non-centrosymmetric hexagonal space group $P\bar{6}2m$ (#189, $a = 7.6357(3)$ Å, $c = 4.4698(3)$ Å, $V = 225.69(2)$ Å^3, $Z = 3$, and $R/wR = 0.0173/0.0268$). NaSrP adopts an ordered Fe_2P structure type. PSr_6 trigonal prisms share trigonal (pinacoid) faces to form 1D chains. Those chains define large channels along the [001] direction through edge-sharing. The channels are filled by chains of PNa_6 face-sharing trigonal prisms. Li_4SrP_2 crystallizes in the rhombohedral space group $R\bar{3}m$ (#166, $a = 4.2813(2)$ Å, $c = 23.437(2)$ Å, $V = 372.04(4)$ Å^3, $Z = 3$, and $R/wR = 0.0142/0.0222$). In contrast to previous reports, LiSrP and LiBaP crystallize in the centrosymmetric hexagonal space group $P6_3/mmc$ (#194, $a = 4.3674(3)$ Å, $c = 7.9802(11)$ Å, $V = 131.82(2)$ Å^3, $Z = 2$, and $R/wR = 0.0099/0.0217$ for LiSrP; $a = 4.5003(2)$ Å, $c = 8.6049(7)$ Å, $V = 150.92(2)$ Å^3, $Z = 2$, and $R/wR = 0.0098/0.0210$ for LiBaP). Li_4SrP_2, LiSrP, and LiBaP can be described as Li_3P derivatives. Li atoms and P atoms make a graphite-like hexagonal layer, $^2_\infty[LiP]^{2-}$. In LiSrP and LiBaP, Sr or Ba atoms reside between $^2_\infty[LiP]^{2-}$ layers to substitute for two Li atoms of Li_3P, while in Li_4SrP_2, Sr substitutes only between every other $^2_\infty[LiP]^{2-}$ layer.

Keywords: A. Phosphide; C. Crystal structure; D. X-ray diffraction

1. Introduction

Mixed anion compounds such as oxynitrides [1–9], halide nitrides [5,10–15], and chalcogenide nitrides [16–20] have attracted recent attention. Although *III*–N–V (*III* = Ga, In; *V* = P, As) compound semiconductors are very important for light-emitting diode (LED) or laser diode applications, there is only one structurally characterized phosphide nitride, Ca_3PN [21]. This compound shows a phase transition at high temperature (1070 K) from the distorted phase (orthorhombic) to the cubic anti-perovskite structure. The substitution of phosphorus for nitrogen within a nitride network may enable band gap tuning, similar to the insertion of nitrogen within an oxide network [22].

Many phosphide materials with various compositions and crystal structures are known [23,24]. Moreover, ternary compounds with simple 1:1:1 composition crystallize in more than 30 different structure types some of which are common to intermetallic phases [25]. NaSrP and Li*Ae*P (*Ae* = Sr, Ba) reported here belong to the ZrNiAl [26] and ZrBeSi [27] structure types, respectively. LiSrP and LiBaP were previously reported to crystallize in a noncentrosymmetric hexagonal $P\bar{6}2m$ space group, based on powder diffraction data [28]. However, in this work, single crystal studies show that these two compounds adopt a centrosymmetric hexagonal $P6_3/mmc$ structure that can be described as a derivative of Li_3P [29].

The title compounds were initially discovered in syntheses designed to explore the existence of compounds containing both nitrogen and phosphorus as an anion. Although we did not identify any of these mixed anion compounds, the title ternary compounds were discovered.

*Corresponding author. Fax: +1 607 255 4137.
E-mail address: fjd3@cornell.edu (F.J. DiSalvo).

0022-4596/$ - see front matter © 2006 Elsevier Inc. All rights reserved.
doi:10.1016/j.jssc.2006.10.033

Here we report the synthesis and structural characterization of NaSrP, Li_4SrP_2, LiSrP, and LiBaP.

2. Experimental section

2.1. Synthesis

All manipulations were performed in an argon-filled glovebox. Single crystals of the title compounds were observed during attempts to prepare a new class of phosphide nitrides by employing Na/Sn metallic alloy or Li_3N fluxes. All chemicals except Ba_2N were used as obtained: NaN_3 (99%, Aldrich), Li_3N (−80 mesh, Aldrich), Sr (filed from rod, 99 + %, Aldrich), Ba (filed from rod, 99 + %, Aldrich), red P (99.999%, JohnsonMatthey), Li (99.9%, Aldrich), Na (ACS reagent, stick, dry, Aldrich), and Sn (99.9%, JohnsonMatthey). Ba_2N was obtained by the reaction of Ba metal with a N_2 gas stream at 850 °C; purity was checked by PXRD. All reactions for the title compounds were carried out in Nb metal tubes, which were welded closed using a Centorr Associates arc furnace. The sealed Nb tubes were jacketed in evacuated silica tubes to protect the tubes from oxidation during heat treatment. Before use, the surfaces of Na and Li metals were scraped clean and Nb tubes were cleaned in a mixture of concentrated H_2SO_4, HNO_3, HF (45:40:15 by volume. *CAUTION*: This solution is extremely corrosive and contact with skin may be fatal.) [30].

NaSrP: The starting materials of 0.0650 g of NaN_3, 0.0876 g of Sr, 0.0310 g of P, 0.0920 g of Na, and 0.1187 g of Sn (atomic ratio of Na/Sr/P/Sn was 5:1:1:1) were loaded into a Nb tube. After the open end of the Nb tube was welded closed in an argon atmosphere, the Nb tube was put into a silica tube and sealed under vacuum to prevent oxidation of the reaction tube during heating. The reaction tube was heated gradually to 600 °C for 24 h and held at this temperature for 120 h. The furnace was turned off and the reaction tube cooled to room temperature over approximately 24 h. After completing the reaction, excess Na was removed by sublimation at 340 °C under dynamic vacuum. Irregular shaped red crystals were found in the reaction mixture.

Li_4SrP_2 and LiSrP: The starting materials of 0.0697 g of Li_3N, 0.0876 g of Sr, 0.0479 g of Ti, and 0.0310 g of P (atomic ratio of Li/Sr/Ti/P was 6:1:1:1) were loaded into a Nb tube, as described above. The reaction tube was heated gradually to 900 °C for 24 h and held at this temperature for 120 h. The furnace was turned off and the reaction tube cooled to room temperature. Irregular shaped red (Li_4SrP_2) and yellow (LiSrP) crystals were found in the reaction mixture.

LiBaP: The starting materials of 0.0522 g of Li_3N, 0.1443 g of Ba_2N, 0.0479 g of Ti, and 0.0310 g of P (atomic ratio of Li/Ba/Ti/P was 9:2:2:2) were weighted into a Nb tube and handled as above. The reaction tube was heated gradually to 900 °C for 24 h and held at this temperature for 120 h. The furnace was turned off and the reaction tube cooled to room temperature. Irregular shaped red crystals were found in the reaction mixture.

2.2. Crystallographic studies

Samples of the reaction mixture were removed from the glovebox in polybutene oil for single-crystal selection. All crystals were manually selected from the reaction mixture, mounted in a drop of polybutene oil sustained in a plastic loop, and placed onto the goniometer within a cold nitrogen stream that froze the polybutene oil thus keeping the crystals stationary and protected from oxygen and moisture in the air. Several crystals were selected for each compound and the unit cell parameters measured to check crystal uniformity.

Preliminary examination and data collection were performed on a Bruker X8 Apex II diffractometer equipped with 4 K CCD detector and graphite-monochromatized Mo $K\alpha$ radiation ($\lambda = 0.7107$ Å). The initial unit cell constants and orientation matrix were obtained by using APEX2 [31]. The program SAINT was used to integrate the data [32]. An empirical absorption correction was applied using SADABS [33]. The initial input files for solving the crystal structure were prepared by XPREP [34]. The initial positions for all atoms were obtained by using direct methods of the SHELXS97 [35] and the structure was refined by full-matrix least-squares techniques with the use of the SHELXL97 [35] in the WinGX program packages [36]. The positional parameters were standardized by using the program STRUCTURE TIDY [37] and refined anisotropically. For all compounds, the distribution of normalized structure factor (E-values, $\langle E^2-1 \rangle = 0.572$ for NaSrP; 0.725 for Li_4SrP_2; 0.504 for LiSrP; 0.460 for LiBaP) suggested that the structures of the title compounds may be noncentrosymmetric. However, we first chose the centrosymmetric space group $R\bar{3}m$ for Li_4SrP_2 and $P6_3/mmc$ for LiSrP and LiBaP and satisfactory refinement confirmed the choice of these space groups. We could not find a good structural solution for NaSrP in any centrosymmetric space group, but only in $P\bar{6}2m$. Additionally, for all compounds, the ADDSYM algorithm in the PLATON program packages could not find any additional symmetry in these structures [38,39].

NaSrP: Of 3789 reflections collected in the θ range 3.08–39.31° using ϕ and ω scans, 520 were unique ($R_{int} = 0.0378$). The final cycle of refinement performed on F_0^2 with 520 unique reflections afforded residuals $wR_2 = 0.0268$ and a conventional R index based on 472 reflections having $F_0^2 > 2\sigma(F_0^2)$ of 0.0173. The highest peak (0.376 e/Å^3) and deepest hole (−0.623 e/Å^3) are located 1.74 and 1.29 Å from Sr and P(2) atoms, respectively, and are due to data truncation errors ($2\theta \approx 80°$).

Li_4SrP_2: Of 2534 reflections collected in the θ range 2.61–43.96° using ϕ and ω scans, 416 were unique ($R_{int} = 0.0235$). The final cycle of refinement performed on F_0^2 with 416 unique reflections afforded residuals $wR_2 = 0.0222$ and a conventional R index based on 411

reflections having $F_0^2 > 2\sigma(F_0^2)$ of 0.0142. The highest peak (0.490 e/Å^3) and deepest hole (−0.408 e/Å^3) are located 0.79 and 1.25 Å from Sr and Li(2) atoms, respectively, and are due to data truncation errors ($2\theta \approx 88^\circ$).

LiSrP: Of 1659 reflections collected in the θ range 5.11–40.34° using ϕ and ω scans, 189 were unique ($R_{int} = 0.0231$). The final cycle of refinement performed on F_0^2 with 189 unique reflections afforded residuals $wR_2 = 0.0217$ and a conventional R index based on 171 reflections having $F_0^2 > 2\sigma(F_0^2)$ of 0.0099. The highest peak (0.293 e/Å^3) and deepest hole (−0.537 e/Å^3) are located 2.03 and 0.85 Å from P and Sr atoms, respectively, and are due to data truncation errors ($2\theta \approx 80^\circ$).

LiBaP: Of 2544 reflections collected in the θ range 4.74–43.76° using ϕ and ω scans, 261 were unique ($R_{int} = 0.0236$). The final cycle of refinement performed on F_0^2 with 261 unique reflections afforded residuals $wR_2 = 0.0210$ and a conventional R index based on 233 reflections having $F_0^2 > 2\sigma(F_0^2)$ of 0.0098. Both highest peak (0.456 e/Å^3) and deepest hole (−0.783 e/Å^3) are located 2.15 and 0.71 Å from atom Ba and are due to data truncation errors ($2\theta \approx 88^\circ$).

2.3. Preparation of bulk samples

After the structure determination, we found that bulk powder samples of the title compounds can be obtained from a stoichiometric mixture of the elements. The starting elements were weighed out in a specific ratio (1:1:1 for *AAe*P and 4:1:2 for Li_4SrP_2) and loaded into Nb tubes. The sealed Nb tubes were sealed inside a silica tubes under vacuum to be protected from oxidation in air during heating. All tubes were heated gradually to 900 °C for 24 h, kept at this temperature for 120 h, and then cooled to room temperature.

Powder X-ray diffraction patterns were subsequently obtained on a Scintag 2000 θ–θ diffractometer with Cu $K\alpha$ radiation. Due to the air sensitivity of all these products, the powder diffraction samples were prepared in an argon-filled glovebox and covered with a Mylar film. PXRD results for each compound show mixtures of products, such as about 20% of $Na_2Sr_3P_4$ [40] in NaSrP, about 18% of LiSrP for Li_2SrP_4, about 11% Li_2SrP_4 in LiSrP, and about 24% of Ba_3P_2 [41] in LiBaP.

2.4. Electronic microprobe analysis

Microprobe analysis of the title compounds were made with an EDAX (Thermonoran) equipped scanning electron microscope (Jeol JXA-8900R). Since the title compounds except Li_4SrP_2 are highly moisture sensitive, the single crystal samples were transferred from an argon-filled glovebox to the microprobe using a specially designed portable antechamber [42] to prevent decomposition of the samples in air. The average atomic ratios were calculated from six data sets obtained from two or three crystals for each compound. Analyses of the crystals indicated the presence of Na, Sr and P in NaSrP (atomic percent: 25.6:44.0:30.4) of Sr and P in Li_4SrP_2 (31.0:69.0), of Sr and P in LiSrP (45.4:54.6), and of Ba and P in LiBaP (50.6:49.4). No other elements, such as Ti, Sn, or Nb, were detected for the title compounds. Since the method is standardless, these analyses are consistent within expected errors with the crystallographically determined composition.

3. Results and discussion

The structures of the title compounds have been determined by single-crystal X-ray diffraction. The site occupancy refinements of P atoms for the title compounds were carried out to confirm the absence of the other impurities. For all compounds, P atoms occupy their own crystallographic sites over 99.5% and the anisotropic displacement parameters are not abnormal. Also WDX spectra show there are no oxygen or nitrogen signals. Those imply that all P sites are ordered with no oxygen or nitrogen impurities. Crystallographic details, fractional atomic coordinates and equivalent isotropic displacement parameters are given in Tables 1 and 2, respectively. Selected bond distances for all the compounds are listed in Table 3.

The crystal structure of NaSrP adopts the ZrNiAl [26], a ternary ordered Fe_2P structure type, in the noncentrosymmetric hexagonal space group $P\bar{6}2m$, with one independent position for Na(3*f*), one for Sr(3*g*), and two for P atoms (2*c* for P(1) and 1*b* for P(2)), and is isostructural with NaBaP [43]. Na atoms are surrounded by four P (two P(1) and two P(2)) atoms in tetrahedron geometry. Sr atoms are encircled by five P atoms in rectangular pyramid geometry. In the Sr-centered P rectangular pyramid, four symmetrically related P(1) atoms are located at each corner of the rectangular plane and a P(2) atom is positioned at the apex. The Na-centered P tetrahedra and Sr-centered P rectangular pyramids share their all edges to make a three-dimensional structures (Fig. 1(a)). Fig. 1(b) emphasizes the trigonal prismatic environment of the P atoms. Both P atoms have nine near neighbors; P(1) with six Sr (3.2039(1) Å) and three Na (2.9579(7) Å) neighbors and P(2) with six Na (2.8984(7) Å) and three Sr (3.1764(3) Å) neighbors. P(1)Sr_6 trigonal prisms share trigonal faces to make a one dimensional chain. Those chains make a large channel along the [001] direction through edge-sharing. These channels are filled by chains of P(2)Na_6 trigonal prisms sharing trigonal faces (Fig. 1(b)). Na–P and Sr–P distances in NaSrP range from 2.8984(7)–2.9579(7) Å and from 3.1764(3) to 3.2039(1) Å, respectively. Those values are in good agreement with those found in binary phosphides Na_3P (2.8586(3)–2.9073(17) Å) [44] and α-SrP_3 (3.030(2)–3.447(2) Å (avg. 3.217 Å)) [45] and are also comparable to those in ternary $Na_2Sr_3P_4$ (Na–P: 2.905(5)–3.531(7) Å; Sr–P: 2.995(3)–3.158(3) Å) [40], NaBaP (Na–P: 3.006–3.095 Å) [43], CuSrP (Sr–P: 3.18 Å) [46], and other Sr-containing compounds, such as LiSrP

Table 1
Details of X-ray data collection and refinement for NaSrP, Li_4SrP_2, LiSrP, and LiBaP

	NaSrP (dark red)	Li_4SrP_2 (red)	LiSrP (yellow)	LiBaP (dark red)
Formula weight, amu	141.58	177.32	125.53	175.25
Space group	$P\bar{6}2m$	$R\bar{3}m$	$P6_3/mmc$	$P6_3/mmc$
a (Å)	7.6357(3)	4.2813(2)	4.3674(3)	4.5003(2)
c (Å)	4.4698(3)	23.437(2)	7.9802(11)	8.6049(7)
V (Å^3)	225.69(2)	372.04(4)	131.82(2)	150.92(2)
Z	3	3	2	2
T (K)	167.0(1)	167.0(1)	167.0(1)	167.0(1)
Linear absorption coefficient (mm^{-1})	18.245	11.313	20.652	13.334
Density, calc. (g/cm^3)	3.125	2.374	3.163	3.856
Crystal size (mm^3)	$0.09 \times 0.06 \times 0.03$	$0.09 \times 0.07 \times 0.07$	$0.09 \times 0.07 \times 0.04$	$0.07 \times 0.07 \times 0.06$
θ limits (deg)	3.08–39.31	2.61–43.96	5.11–40.34	4.74–43.76
No. of unique data with F_0^2	520 [R(int) = 0.0378]	416 [R(int) = 0.0235]	189 [R(int) = 0.0231]	261 [R(int) = 0.0236]
No. of unique data with $F_0^2 > 2\sigma(F_0^2)$	472	411	171	233
wR_2 ($F_0^2 > 0$)	0.0268	0.0222	0.0217	0.0210
$R1$ (on F_0 for $F_0^2 > 2\sigma(F_0^2)$)	0.0173	0.0142	0.0099	0.0098
Goodness-of-fit on F^2	0.796	1.114	1.079	1.131
Flack parameter	0.021(7)			
Max. and min. residual e-density(e/Å^3)	0.376 and −0.623	0.490 and −0.408	0.293 and −0.537	0.456 and −0.783

Table 2
Atomic coordinates and equivalent isotropic displacement parameters (Å^2) for NaSrP, Li_4SrP_2, LiSrP, and LiBaP

Atoms	Wyckoff notation	x	y	z	U_{eq}[a]
NaSrP					
Na	3f	0.7583(1)	0	0	0.009(1)
Sr	3g	0.4160(1)	0	0.5000	0.007(1)
P(1)	2c	0.6667	0.3333	0	0.006(1)
P(2)	1b	0	0	0.5000	0.007(1)
Li_4SrP_2					
Li(1)	6c	0	0	0.1377(1)	0.012(1)
Li(2)	6c	0	0	0.4291(1)	0.012(1)
Sr	3a	0	0	0	0.006(1)
P	6c	0	0	0.2463(1)	0.006(1)
LiSrP					
Li	2c	0.3333	0.6667	0.2500	0.016(1)
Sr	2a	0	0	0	0.006(1)
P	2d	0.3333	0.6667	0.7500	0.005(1)
LiBaP					
Li	2c	0.3333	0.6667	0.2500	0.012(1)
Ba	2a	0	0	0	0.007(1)
P	2d	0.3333	0.6667	0.7500	0.007(1)

[a] U_{eq} is defined as one-third of the trace of the orthogonalized U_{ij} tensor.

(3.2153(2) Å) and Li_4SrP_2 (3.2053(2) Å) described this paper.

Previously, LiSrP and LiBaP were reported to adopt the SrPtSb structure type in the noncentrosymmetric space group $P\bar{6}2m$ through powder X-ray work [28]. In that report, there is only one formula unit with half the c-axis reported here (3.991(1) Å for LiSrP; 4.303(1) Å for LiBaP). The extinction conditions ($hh2\bar{h}l$: $l = 2n$; 000l: $l = 2n$) are missed due to the low intensity of the powder data. In some cases, a determination of the correct structure solely on the basis of powder X-ray data is not possible. From the single crystal studies, LiSrP and LiBaP crystallize in the centrosymmetric hexagonal space group $P6_3/mmc$ with two formula units and the c-axis double that proposed from powder diffraction (see Table 1). Sr^{2+} or Ba^{2+} atoms sit on positions with $\bar{3}m$ symmetry, while Li^+ and P^{3-} atoms occupy sites of $\bar{6}2m$ symmetry. LiSrP and LiBaP adopt the ZrBeSi [27] structure type and also can be described as Li_3P [29] derivatives. The structure of LiSrP and LiBaP is made up of alternate graphite-like anionic layers of $^2_\infty[LiP]^{2-}$ which extended along the crystallographic ab plane, while Sr^{2+} or Ba^{2+} cations reside

Table 3
Selected bond lengths [Å] and angles [deg] for NaSrP, Li_4SrP_2, LiSrP, and LiBaP

NaSrP			
Na–P(1) × 2	2.9579(7)	Sr–P(1) × 4	3.2039(1)
Na–P(2) × 2	2.8984(7)	Sr–P(2)	3.1764(3)
P(1)–Na–P(2) × 4	115.124(2)	P(1)–Sr–P(2) × 4	101.550(4)
P(1)–Na–P(1)	96.35(3)	P(1)–Sr–P(1) × 2	156.901(8)
P(2)–Na–P(2)	100.90(3)	P(1)–Sr–P(1) × 4	86.942(4)
Li_4SrP_2			
Li(1)–P	2.545(3)	Li(1)-Li(1)	2.821(2)
Li(1)–P × 3	2.742(1)	Li(1)–Li(2)	2.660(1)
Li(2)–P × 3	2.4802(3)	Sr–P × 6	3.2053(2)
P–Li(1)–P × 3	115.63(5)	P–Sr–P × 3	180.0
P–Li(1)–P × 3	102.67(6)	P–Sr–P × 6	83.802(7)
P–Li(2)–P × 3	119.33(2)	P–Sr–P × 6	96.198(7)
LiSrP			
Li–P × 3	2.5215(2)	Sr–P × 6	3.2153(2)
Li–Sr × 6	3.2153(2)		
P–Li–P × 3	120.0	P–Sr–P × 3	180.0
		P–Sr–P × 6	85.555(6)
		P–Sr–P × 6	94.445(6)
LiBaP			
Li–P × 3	2.5983(1)	Ba–P × 6	3.3732(1)
Li–Ba × 6	3.3732(1)		
P–Li–P × 3	120.0	P–Ba–P × 3	180.0
		P–Ba–P × 6	83.681(4)
		P–Ba–P × 6	96.319(4)

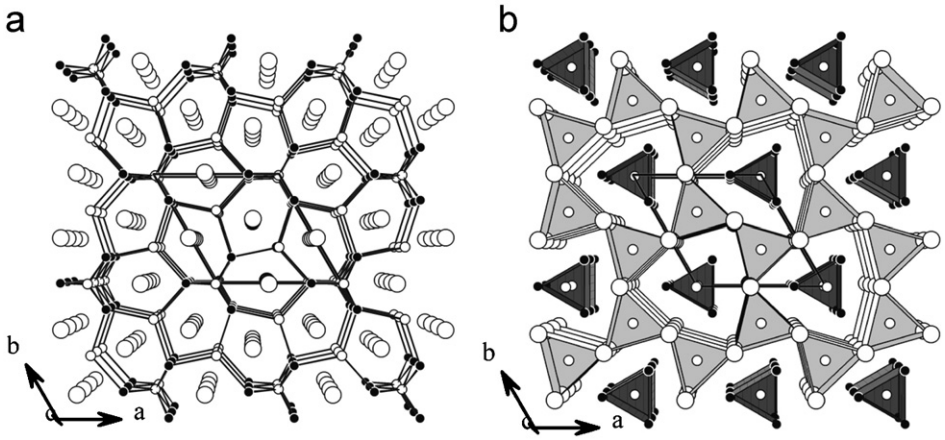

Fig. 1. (a) Perspective view of NaSrP along the [001] direction. (b) P-centered trigonal prismatic view along the [001] direction. P(1)Sr_6 tigonal prisms are light gray and P(2)Na_6 trigonal prisms are dark gray. For both figures, bonds between Sr and P atoms for (a) and capped P-Na or P–Sr for (b) were omitted for clarity. Large open circles are Sr atoms, small filled circles are Na atoms, and small open circles are P atoms.

between the anionic $^2_\infty[LiP]^{2-}$ layers (Fig. 2(a)). Between the layers, Sr^{2+} and Ba^{2+} cations are surrounded by six Li and six P atoms in a hexagonal prism. These hexagonal prisms share their all rectangular faces along the *ab* plane and all hexagonal faces along the *c*-axis. P atoms are bounded by six Sr or Ba atoms and three Li atoms in tricapped trigonal prismatic geometry (Fig. 2(b)). Li–P distances are 2.5215(2) Å for LiSrP and 2.5983(1) Å for LiBaP. Those values are somewhat longer than those of Li_3P (2.462 Å). Since large Sr^{2+} or Ba^{2+} cations substitute for the smaller Li^+ cations in Li_3P, the Li_3P_3 hexagon (the angles of Li–P–Li and vice versa are ideally 120°) widen along the *ab* plane. Sr–P and Ba–P distances are 3.2153(2) Å for LiSrP and 3.3732(1) Å for LiBaP. The Sr–P distance is in good agreement with the above mentioned compounds and the Ba–P distance is comparable to those in the binary α-Ba_5P_4 (3.189(3)–3.293(3) Å) [47] and ternary NaBrP (3.293–3.343 Å) [43].

Li_4SrP_2 crystallizes in the centrosymmetric rhombohedral space group $R\bar{3}m$, with two independent positions for

Li (3*m*), one for Sr ($\bar{3}m$), and one for P atoms (3*m*). The crystal structure is composed of alternate graphite-like anionic layers of $^{2}_{\infty}[Li(2)P]^{2-}$ which extended along the crystallographic *ab* plane while the remaining Li(1) and Sr atoms lie between anionic $^{2}_{\infty}[Li(2)P]^{2-}$ layers. Li(1) and Sr atoms lying between anionic $^{2}_{\infty}[Li(2)P]^{2-}$ layers are coordinated to four P atoms arranged in a distorted tetrahedral geometry and six P and six Li(2) atoms arranged in a hexagonal prism, respectively. Alternatively, the crystal structure of Li_4SrP_2 can be described as intergrowth of Li_3P and LiSrP layers (Fig. 3(a)). In the Li_3P layer (A layer), two Li atoms are sandwiched between the anionic $^{2}_{\infty}[LiP]^{2-}$ layers as in Li_3P [29]. In the LiSrP layer (B layer), the Sr atom has same geometry as in LiSrP and anionic $^{2}_{\infty}[LiP]^{2-}$ layers are staggered as found in Li*Ae*P (see Fig. 2(b)). As shown in Fig. 3(a), both layers are stacked (…ABA′B′A″B″A…) along the *c*-axis and slide a little bit along the *ab* plane to make the large *c* cell parameter. Li(1)-P distances in the $Li(1)P_4$ tetrahedron range from 2.545(3)–2.742(1) Å and Li(2)–P distance in the $^{2}_{\infty}[Li(2)P]^{2-}$ layer is 2.4802(3) Å. Those values are in good agreement with Li_3P (2.524–2.768 Å in the LiP_4 tetrahedra and 2.462 Å in the $^{2}_{\infty}[LiP]^{2-}$ layer). The smaller Sr substitution between the LiP layers results in less steric expansion of the Li_3P_3 hexagon. The Sr–P distance is 3.2053(2) Å which is in good agreement with above mentioned Sr-containing compounds. P atoms are bounded by seven lithium and three strontium atoms in a tetracapped trigonal prism (Fig. 3(b)). Three Li atoms capping through rectangular faces come from the

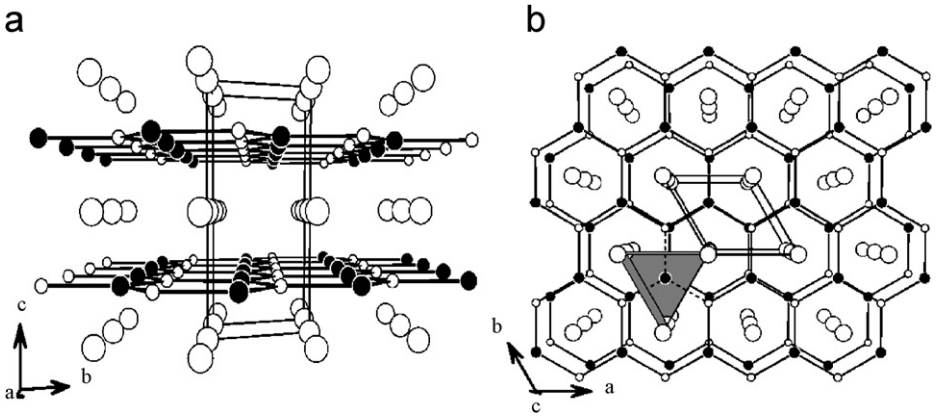

Fig. 2. (a) The crystal structure of Li*Ae*P (*Ae* = Sr, Ba) along the [100] direction. (b) Perspective view of Li*Ae*P (*Ae* = Sr, Ba) along the [001] direction. The environment of the P atom is highlighted by a polyhedron drawing. Large open circles are Sr or Ba atoms, small open circles are Li atoms, and medium filled circles are P atoms.

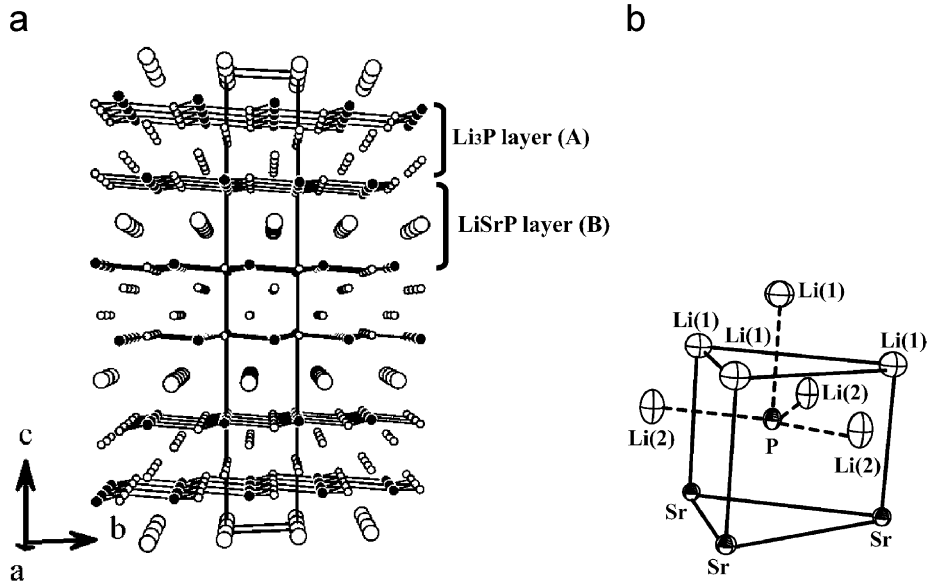

Fig. 3. (a) The crystal structure of Li_4SrP_2, represented by Li_3P and LiSrP layers, along the [100] direction. Large open circles are Sr atoms, small open circles are Li atoms, and medium filled circles are P atoms. (b) The tetracapped trigonal prismatic environment of the P atom. Displacement ellipsoids are drawn at the 90% probability level.

$^2_\infty$[Li(2)P]$^{2-}$ layer and the one Li atom capping through the triangular face and the three Li atoms in the triangular face come from Li(1) layer.

LiSrP, LiBaP, and Li_4SrP_2 can be described as Li_3P derivatives as mentioned above. Sr^{2+} or Ba^{2+} cations substitute for two Li^+ cations ($Li_2[LiP] \rightarrow Ae[LiP]$ (Ae = Sr, Ba); $2Li_2[LiP] \rightarrow Li_2Sr[LiP]_2$). While Ae^{2+} cations in LiSrP and LiBaP substitute for all interlayer Li, Sr^{2+} cations in Li_4SrP_2 substitute half of the Li_2 layers. Since the substituted Sr^{2+} (1.44 Å) or Ba^{2+} (1.61 Å) cations are larger than Li^+ (0.76 Å) [48], full or partial substitutions produce a 1:1:1 phase for LiSrP and LiBaP and a structural modification for Li_4SrP_2. Consequently, as the size of metals between the anionic $^2_\infty$[LiP]$^{2-}$ layers increases, the unit cell constants and interlayer distance between anionic $^2_\infty$[LiP]$^{2-}$ layers increase almost linearly as shown in Fig. 4. In Li_4SrP_2 the interlayer distance between the anionic $^2_\infty$[Li(2)P]$^{2-}$ layers is much smaller than in the Li_3P binary (3.323 vs 3.789 Å, respectively), while the interlayer distance in the LiSrP layer is larger than that of LiSrP (4.285 vs 3.990 Å, respectively). Interestingly, the size of the $^2_\infty$[LiP]$^{2-}$ net hardly changes on going from Li_3P to Li_4SrP_2 (the a-axis increases from 4.264 to 4.2813 Å, respectively), while the a-axis of LiSrP is much larger (4.3674 Å).

The bond valence sums and Madelung site potentials were calculated with the program EUTAX [49] and the results are listed in Table 4. The default values of the R_{ij} (Na–P = 2.360; Li–P = 2.040; Sr–P = 2.670; Ba–P = 2.880) for cation–anion single bonds were used to calculate the bond valence sums. The Madelung potentials were determined by assigning ionic charges for all atoms (Na^+, Li^+, Sr^{2+}, Ba^{2+}, P^{3-}). The calculated valence sums for an atom in purely ionic compounds are expected to be close to their valence and normally calculated site potentials are close to −10 times the formal charge of ion [50]. However, the calculated bond valence sums and Madelung site potentials shown in Table 4 are all systematically low. This may be due to the covalent character of the bonding compared to halides, oxides, or even nitrides. The electronegativity of P (Mulliken EN = 2.30) is much less than that of the neighboring elements (usual anions) such as N (2.90), S (2.69), C (2.48), and O (3.41) [51]. The color (red or yellow) of each compound also suggests that the title compounds are closed shell semiconductors with a relatively large optical band gap. The classical charge valences can thus be described as [Na^+ or Li^+][Sr^{2+} or Ba^{2+}][P^{3-}] for 1:1:1 phases and [Li^+]$_4$[Sr^{2+}][P^{3-}]$_2$ for the 4:1:2 phase, as expected for simple insulators.

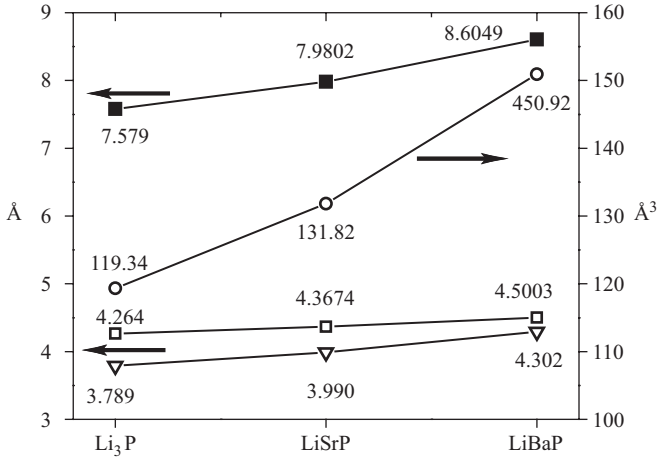

Fig. 4. Comparison of the unit cell parameters and anionic interlayer distances. (□: a-axis, ■: c-axis, ○: unit cell volume, ▽: interlayer distance).

Table 4
Calculated Bond Valence Sums and Madelung Site Potentials of NaSrP, Li_4SrP_2, LiSrP, and LiBaP

	Atoms	Bond valence sum	Madelung site potential (V)
NaSrP	Na	0.86	−9.60
	Sr	1.12	−15.3
	P(1)	2.01	23.4
	P(2)	2.16	23.2
Li_4SrP_2	Li(1)	0.71	−9.72
	Li(2)	0.91	−10.7
	Sr	1.41	−15.1
	P	2.33	25.5
LiSrP	Li	0.82	−11.1
	Sr	1.37	−15.4
	P	2.19	24.5
LiBaP	Li	0.67	−11.0
	Ba	1.61	−14.7
	P	2.28	23.4

4. Summary

Four phosphides, NaSrP, LiSrP, LiBaP, and Li_4SrP_2, have been obtained in attempts to prepare new phosphide nitrides and structurally characterized by single crystal X-ray diffraction techniques. The previously reported structures of LiSrP and LiBaP have been corrected and experimentally proved to be in the centrosymmetric space group $P6_3/mmc$. The results presented here and other results [44,52,53] clearly demonstrate that phosphides are thermodynamically favorable rather than nitride or phosphide nitride compounds. Also it can be expected that many more new and interesting phosphides will be accessible by a systematic variation of the present reaction conditions. Although we did not attempt to prepare unknown analogous, such as KAeP (Ae = alkaline earth metals) or 4:1:2 series compounds, with the same structure type, further study in this area is warranted.

5. Supporting information

The crystallographic files in CIF format for the title compounds have been deposited with FIZ Karlsruhe as CSD no. 416887 for NaSrP, 416888 for Li_4SrP_2, 416889 for LiSrP, and 416890 for LiBaP. The data may be obtained

free of charge by contacting FIZ Karlsruhe at +49 7247 808 666 (fax) or crysdata@fiz–karlsruhe.de (email).

Acknowledgments

This work was supported in part by the National Science Foundation through Grant DMR-0602526. We really appreciate Prof. Wolfgang Jeitschko at University of Müenster for his helpful discussion. We also thank Dr E. Lobkovsky (single-crystal diffraction) and J. Hunt (SEM microprobe) for the use of their facilities at Cornell University. The SEM microprobe is one of the Cornell Center for Materials Research Shared Experimental Facilities, supported through the National Science Foundation Materials Research Science and Engineering Center Program (DMR-0520404).

References

[1] A. Lieb, W. Schnick, Solid State Sci. 8 (2006) 185–191.
[2] H.A. Höppe, F. Stadler, O. Oeckler, W. Schnick, Angew. Chem. Int. Ed. 43 (2004) 5540–5542.
[3] C.W. Michie, J.B. Claridge, S.J. Clarke, M.J. Rosseinsky, Chem. Mater. 15 (2003) 1547–1553.
[4] R. Marchand, Y. Laurent, J. Guyader, P. L'Haridon, P. Verdier, J. Eur. Ceram. Soc. 8 (1991) 197–213.
[5] R. Niewa, F.J. DiSalvo, Chem. Mater. 10 (1998) 2733–2752.
[6] M. Pérez-Estébanez, R. Pastrana-Fábregas, J. Isasi-Marín, R. Sáez-Puche, J. Mater. Res. 21 (2006) 1427–1433.
[7] Y.Q. Li, G. de With, H.T. Hintzen, J. Mater. Chem. 15 (2005) 4492–4496.
[8] A. Kasahara, K. Nukumizu, G. Hitoki, T. Takata, J.N. Kondo, M. Hara, H. Kobayashi, K. Domen, J. Phys. Chem. A 106 (2002) 6750–6753.
[9] M. Jansen, H.P. Letschert, Nature 404 (2000) 980–982.
[10] A. Bowman, R.I. Smith, D.H. Gregory, J. Solid State Chem. 197 (2006) 130–139.
[11] O. Reckeweg, F.J. DiSalvo, Solid State Sci. 4 (2002) 575–584.
[12] G.M. Ehrlich, M.E. Badding, N.E. Brese, S.S. Trail, F.J. DiSalvo, J. Alloys Compd. 206 (1994) 95–101;
G.M. Ehrlich, M.E. Badding, N.E. Brese, S.S. Trail, F.J. DiSalvo, J. Alloys Compd. 235 (1996) 133–134.
[13] L. Zhu, M. Ohashi, S. Yamanaka, Chem. Mater. 14 (2002) 4517–4521.
[14] C. Felser, R. Seshadri, J. Mater. Chem. 9 (1999) 459–464.
[15] S. Yamanaka, K.-I. Hotehama, H. Kawaji, Nature 392 (1998) 580–582.
[16] F. Lissner, T. Schleid, J. Alloys Compd. 418 (2006) 68–72.
[17] F. Lissner, T. Schleid, Z. Anorg. Allg. Chem. 632 (2006) 1167–1172.
[18] F. Lissner, T. Schleid, Z. Anorg. Allg. Chem. 631 (2005) 1119–1124.
[19] F. Lissner, T. Schleid, Z. Anorg. Allg. Chem. 629 (2003) 1027–1032.
[20] T. Schleid, Eur. J. Solid State Inorg. Chem. 33 (1996) 227–240.
[21] M.Y. Chern, D.A. Vennos, F.J. DiSalvo, J. Solid State Chem. 96 (1992) 415–425.
[22] F. Cheviré, F. Tessier, R. Marchand, Eur. J. Inorg. Chem. (2006) 1223–1230.
[23] R. Pöttgen, W. Hönle, H.G. von Schnering, in: R.B. King (Ed.), Encyclopedia of Inorganic Chemistry, second ed, Wiley, Chichester, UK, 2005.
[24] M.G. Kanatzdis, R. Pöttgen, W. Jeitschko, Angew. Chem. Int. Ed. 44 (2005) 6996–7023.
[25] M.L. Fornasini, F. Merlo, J. Alloys Compd. 219 (1995) 63–68.
[26] P.I. Krypyakevich, V.Ya. Markiv, Ya. Melnyk, Dopov. Akad. Nauk. Ukr. RSR, Ser. A (1967) 750–753.
[27] J.W. Nielsen, N.C. Baenziger, Acta Crystallogr 7 (1953) 132–133.
[28] J.H. Albering, T. Ebel, W. Jeitschko, Z. Crystallogr. 12 (Suppl.) (1997) 242.
[29] G. Brauer, E. Zintl, Z. Phys. Chem. B 37 (1937) 323–352.
[30] N.N. Greenwood, A. Earnshaw, Chemistry of the Elements, second ed, Butterworth-Heinemann, UK, 1997.
[31] Bruker, APEX2 (version 1.22): Software for the CCD System; Bruker Analytical X-ray System: Madison, WI, 2004.
[32] Bruker, SAINT *Plus*: Software for the CCD System; Bruker Analytical X-ray System: Madison, WI, 2003.
[33] G.M. Sheldrick, SADABS, Institute für Anorganische Chemie der Universität Göttingen, Göttingen, Germany, 2003.
[34] Bruker, XPREP (version 6.14): Bruker Analytical X-ray System: Madison, WI, 2003.
[35] G.M. Sheldrick, *SHELX97*, Program for Crystal Structure Analysis, University of Göttingen, Göttingen, Germany, 1998.
[36] L.J. Farrugia, J. Appl. Crystallogr. 32 (1999) 837–838.
[37] L.M. Gelato, E. Parthé, J. Appl. Crystallogr. 20 (1987) 139–143.
[38] Y. Le Page, J. Appl. Crystallogr. 20 (1987) 264–269;
Y. Le Page, J. Appl. Crystallogr. 21 (1988) 983–984.
[39] A.L. Spek, PLATON. A Multipurpose Crystallographic Tool, Utrecht University, Utrecht, The Netherlands, 1999.
[40] W. Hönle, J. Lin, M. Hartweg, H.G. von Schnering, J. Solid State Chem. 97 (1992) 1–9.
[41] K.E. Maass, Z. Anorg. Allg. Chem. 374 (1970) 11–18.
[42] G.M. Ehrlich, Ph. D. Thesis, Cornell University, Ithaca, NY, 1995.
[43] W. Carrillo-Cabrera, M. Somer, E.-M. Peters, K. Peters, H.G. von Schnering, Z. Kristallogr. 211 (1996) 191.
[44] Y. Dong, F.J. DiSalvo, Acta Crystallogr. E 61 (2005) i223–i224.
[45] X. Chen, L. Zhu, S. Yamanaka, J. Solid State Chem. 173 (2003) 449–455.
[46] A. Mewis, Z. Naturforsch. 33b (1978) 983–986.
[47] G. Derrien, M. Tillard, A. Manteghetti, C. Belin, Z. Anorg. Allg. Chem. 629 (2003) 1601–1609.
[48] R.D. Shannon, Acta Crystallogr. A 32 (1976) 751–767.
[49] N.E. Brese, M. O'Keeffe, Acta Crystallogr. B 47 (1991) 192–197.
[50] N.E. Brese, M. O'Keeffe, Struct. Bond. 79 (1992) 307–379.
[51] Webelements (2006). URL: 〈http://www.webelements.com/〉.
[52] $Na_{15}Ge_8SnP$, Y. Dong, F.J. DiSalvo, manuscript in preparation.
[53] Y. Dong, C. Ranjan, F. J. Disalvo, J. Alloys Compd., in press.